Hindawi Publishing Corporation
EURASIP Journal on Wireless Communications and Networking
Volume 2010, Article ID 254345, 11 pages
doi:10.1155/2010/254345

Research Article

Novel Received Signal Strength-Based Indoor Location System: Development and Testing

Yuri Álvarez, María Elena de Cos, José Lorenzo, and Fernando Las-Heras

Área de Teoría de la Señal y Comunicaciones, Universidad de Oviedo, Edificio Polivalente, Módulo 8, Campus Universitario de Gijón, 33203 Gijón, Spain

Correspondence should be addressed to Yuri Álvarez, yurilope@gmail.com

Received 29 January 2010; Revised 9 May 2010; Accepted 13 July 2010

Academic Editor: Davide Dardari

A received signal strength- (RSS-)-based indoor location method (ILS) for person/assets location in indoor scenarios is presented in this paper. Theoretical bases of the method are the integral equations relating the electromagnetic (EM) fields with their sources, establishing a cost function relating the measured field at the receivers and the unknown position of the transmitter. The aim is to improve the EM characterization of the scenario yielding in a more accurate indoor location method. Regarding network infrastructure implementation, a set of receivers are deployed through the coverage area, measuring the RSS value from a transmitter node which is attached to the asset to be located. The location method is evaluated in several indoor scenarios using portable measurement equipment. The next step has been the network hardware implementation using a wireless sensor network: for this purpose, ZigBee nodes have been selected. Finally, RSS measurements variability due to multipath effects and nonline-of-sight between transmitter and receiver nodes is mitigated using calibration and a correction based on the difference between the free space field decay law and the measured RSS.

1. Introduction

A great amount of research has been carried out for many years about the problem of location estimation due to its enormous importance for many engineering fields. The growth of short-range wireless communication networks, both for personal or industrial purposes, as well as the compatibility between network devices (WiFi-certified), has contributed to the development of radiodetermination methods for indoor environments. Different wireless networking techniques have been proposed as infrastructure [1]: for example, IrDA [2–4], WLAN [5, 6], Bluetooth [7], Ultra Wide-Band (UWB) [8–10], and ZigBee [11].

With respect to the indoor signal propagation, the main problems that the indoor location systems (ILSs) have to overcome are the following [1]:

(a) Signal reflection in the obstacles, that supposes multipath contributions in the radio-frequency (RF) location system sensors.

(b) Signal attenuation when passing through the obstacles placed between the RF transmitters (Tx) and receivers (Rx) [12].

(c) The noise level, that may seriously affect the system performance. It may be critical in ILS due to the low emitted power regarding battery savings in the location network nodes.

(d) The presence of other devices working at the same frequency band may interfere with the sensor network.

Concerning ILS design, it will be influenced by various application requirements such as location network scalability, energy efficiency, and location accuracy [1].

Indoor RF-based ILSs can be classified in three main groups depending on the parameter that is used to determine the position:

(a) time-of-fly (ToF) methods, based on the signal propagation time between the Tx and Rx nodes.

Table 1: Comparison of several ILS accuracy.

Method	Scenario's size (m × m)	Absolute error (m)	Relative error (%)
Ecolocation [15]	7.9 × 14.9	3.0 #1	20.4
MoteTrack [16]	41.8 × 41.8	4.0	9.5
Probability Grid [17]	125 × 125 #2	87.5−100 #2	70−80 #2
MLE [18]	8 × 9	1.8 #1	20

#1 Averaged error.
#2 Outdoor deployment.

ToF methods include: time-of-arrival (ToA), time-difference-of-arrival (TDoA),

(b) angle-of-arrival (AoA) techniques, where the position is estimated by means of the knowledge of the direction of arrival of the signal in the receivers,

(c) received signal strength (RSS) methods, which are founded on the decay law of the received signal versus the distance.

ToA and TDoA methods require the use of ultra wideband (UWB) devices in order to achieve enough temporal resolution, so that the echoes corresponding to reflected signals can be identified and suppressed [8–10]. There are some distinctive advantages of short-range UWB: high immunity to interference from other radio systems, high multipath immunity, high data rate, and accurate resolution capability. Despite UWB methods are more accurate than those ones based on RSS measurements, the network infrastructure is more expensive [1].

Apart from being technically less complex (and hence, less expensive), another advantage of RSS methods with respect to ToF ones is the possibility of using existing wireless infrastructures, for example, WLAN access points [5, 6]. However, RSS methods accuracy is limited by the signal level fluctuations due to multipath contributions that occur in indoor scenarios. Moreover, it must be taken into account that most of the existing wireless devices (e.g., WLAN access points, ZigBee nodes, etc.) have not been designed for an accurate RSS measurement, increasing the measured values uncertainty.

With regards to the indoor scenario's characteristics, the presence of obstacles and walls may obstruct the line-of-sight (LOS) between location network nodes. Some of the mentioned ILSs are often designed to work at frequency bands where LOS between the transmitter and the receiver is required. Then, a high number of receivers and repeaters is typically necessary to ensure the LOS condition [13]. This requirement comes from the signal attenuation effect when passing through objects and walls [12], as well as the need of compensating the measurements distortion due to multipath effects on each network node.

In this sense, it is necessary to remark that, according to a comparison between commercially available sensor nodes supporting TDoA and RSS [14], RSS-based methods can be advantageous in a crowded area where the direct links between a target node and reference nodes are frequently shadowed by walking people. Thus, an RSS method would be enough to fulfill the location requirements depending on the requested accuracy.

The following contribution describes an RSS-based indoor location method for assets location and tracking in industrial warehouses. The method must fulfill an accuracy requirement which is around 5% of the indoor scenario's size. The location algorithm, it is based on the establishment of a cost function having the electric field measurements in a set of Rx as inputs, and being the unknown the Tx node position. This Tx node will be attached to the asset to be located/tracked. Aiming to improve the method accuracy, which is limited by the use of a free-space field propagation model, multicarrier information can be considered.

Regarding hardware infrastructure, ZigBee, a new industrial standard for ad hoc networks based on IEEE 802.15.04 PHY and MAC [15], has been chosen due to its features which makes it suitable for low data rate, low power, and cost-effective wirelessly networked products. Expected applications for ZigBee include remote monitoring, home control, industrial automation, and localization.

The most widely used ZigBee frequency band is $f = 2.400$–2.483 GHz. The specification for network and higher layers are defined by the ZigBee Alliance [16]. Due to the RSS-based localization topic attractiveness, the research community in wireless sensor networks (WSN) has studied and proposed several algorithms. A few of them have been evaluated on a real sensor network using a low-power wireless radio: Ecolocation [17], MoteTrack [18], Probability Grid [19], and maximum likelihood estimator (MLE) [20]. Most of them exhibit similar performance (under similar testing conditions, for example, indoor environment) regarding indoor location accuracy requirements, as shown in Table 1.

Compared to similar RSS-based techniques, the main contributions of the proposed method to be pointed out are:

(1) proposal of a new model relating measured RSS values and free-space field decay law that takes into account the near field terms,

(2) combination of multifrequency information, subject to the hardware infrastructure capabilities (e.g., the selected ZigBee nodes do not support this feature),

(3) scenario division in cells, collecting RSS information in a central point inside each cell. These RSS values are used to calibrate the proposed location method.

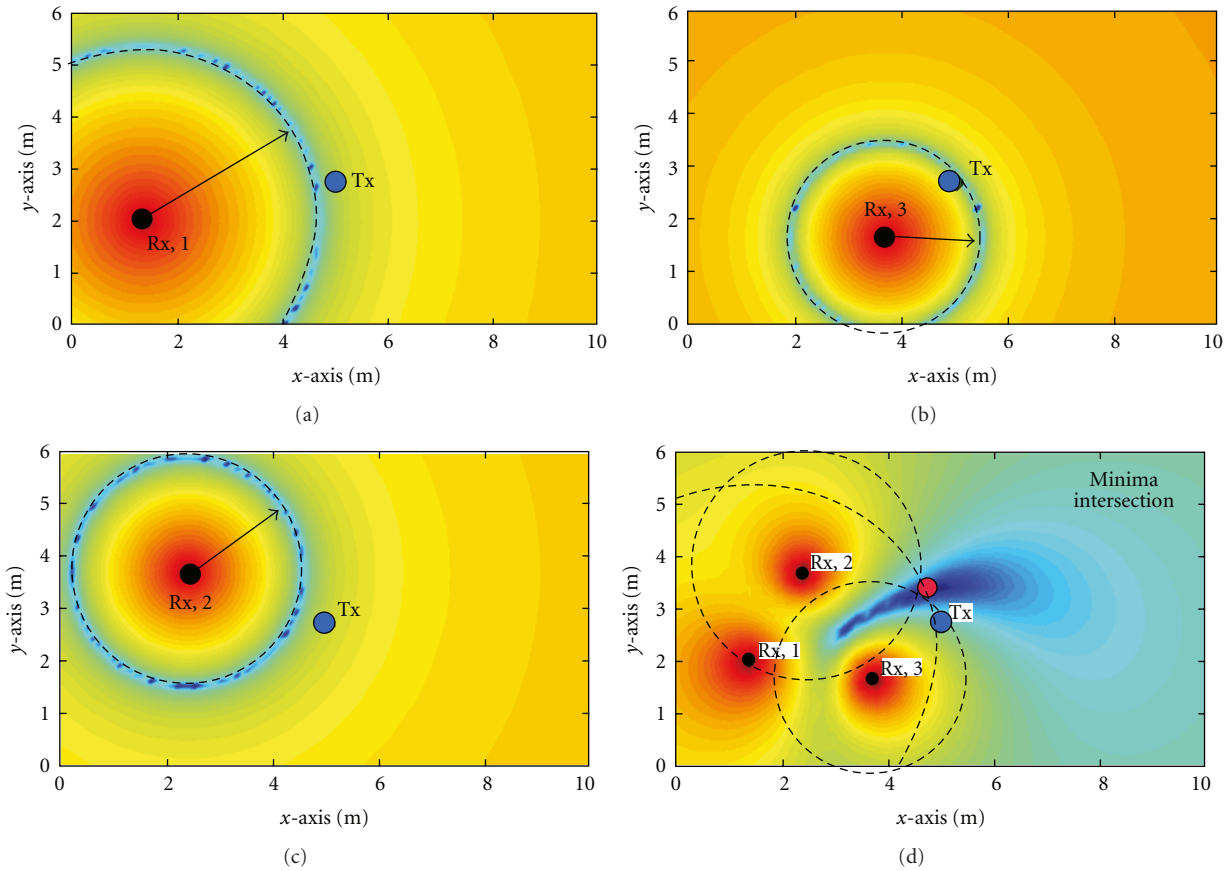

FIGURE 1: Cost function representation for each Rx ($M_{\text{Rx}} = 3$) and combination of the 3 cost functions for estimating the Tx position. Blue color represents the cost function minimum.

2. Description of the Method

2.1. Electromagnetic Propagation Model. Most of the RSS methods are based on the field level decay, which depends on the Tx-Rx distance as:

$$E_{\text{Rx}} = E_0\left(\frac{\lambda}{4\pi R}\right), \tag{1}$$

where E_0 is the field (or signal) level at the Tx node, E_{Rx}, the field level at the Rx, λ is the wavelength ($\lambda = c/f$), and R is the Tx-Rx distance [21].

Equation (1) supposes free-space and far-field conditions. Sometimes, due to the working frequency (f) and the Tx-Rx distance (R), near-field terms (field decaying as $1/R^2$ and $1/R^3$) should be taken into account to avoid loss of accuracy.

Thus, a near-field model is proposed, taking into account the following simplifications: first, the Tx is assumed to be a Hertz dipole (z-polarized, current J_z). Second, Tx and Rx are placed at the same height, so the electric field is also z-polarized. Hence, the equation relating E_{Rx} and E_0 is, in an unbounded medium [21], given by:

$$E_{\text{Rx}} = \frac{-j\eta}{4\pi k_0} E_0\left(\frac{-1 - jk_0R + k_0^2R^2}{R^3}\right)e^{-jk_0R}, \tag{2}$$

η is the intrinsic impedance, and k_0, the wavenumber.

Theoretically, (1) and (2) are valid for free-space conditions. However, it will be shown that they still provide accurate location results in moderate multipath environments.

2.2. Tx Position Determination. Given all the equation parameters, the unknowns defining the Tx position are the cartesian coordinates (x', y'). From (2), the following cost function is established:

$$f_{\text{cost}} = \sum_{m=1}^{M_{\text{Rx}}}\sum_{n=1}^{N_{\text{freq}}}\left|\underbrace{\left|E^{f_n}_{\text{Rx}_m(x,y)}\right|}_{\text{MEAS}} - \underbrace{\left|E_{J,z}(x', y', f_n, R_{x_m(x,y)})\right|}_{\text{EST}}\right|^2, \tag{3}$$

where MEAS is the amplitude of the measured electric field at each Rx ($\text{Rx}_{m(x,y)}$) for each carrier (f_n). The cost function is established as the difference between the measured value and the evaluation of (2) at different positions (x', y') inside the indoor scenario (EST term). M_{Rx} is the number of Rx nodes, and N_{freq} is the number of carriers.

The next step is the cost-function minimization (3) in order to retrieve the (x', y') values corresponding to the Tx position. For each mth Rx, the cost function has the behavior plotted in Figure 1: the Tx placement corresponds to the circumference containing the cost function minimum

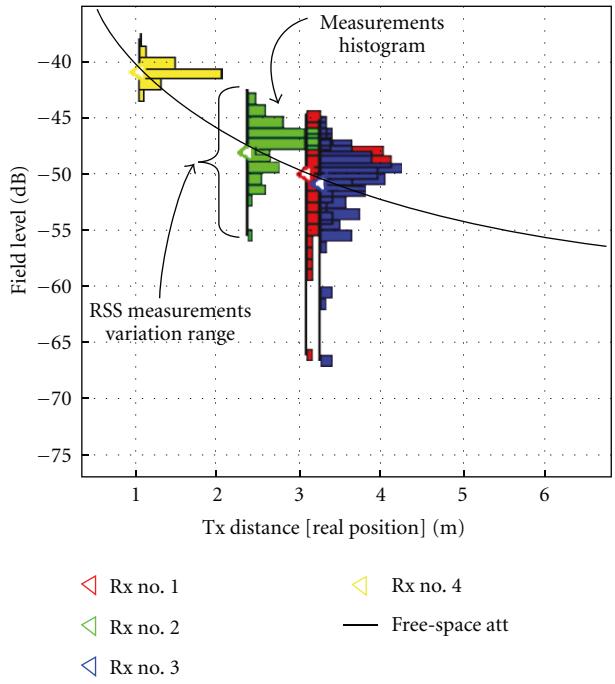

Figure 2: Measured RSS histogram at each Rx, and deviation with respect to the free-space decay law (black line).

value (dashed black line in Figure 1). Under the assumption of ideal free-space propagation, the intersection of three circles will provide the point where the Tx is placed (red dot in Figure 1), as illustrated in [22]. However, deviation of the measured RSS values from the free space field decay law (see Figure 2) introduces some error in the circular minima, being necessary to increase the number of Rx (M_{Rx}) to ensure an accurate Tx position estimation.

The cost function defined in (3) is nonlinear with respect to the unknowns (x', y'), being suitable to be solved using nonlinear optimization techniques (Newton-Raphson [23], Levenberg-Marquardt [23]). However, RSS measurements are affected by multipath effects or attenuation when passing through walls, distorting them from the expected free space values. The result is that the cost function may have local minima, where the mentioned minimization methods [23] can be trapped.

Taking into account these aspects, it is proposed a cost function minimization based on a best-effort method: the domain is divided using a $\Delta x', \Delta y'$ grid; the cost function is evaluated at each point of the grid (x', y'); the Tx position estimation corresponds to the point where the cost function has the lowest value [24, 25].

2.3. Location Method Calibration. The E_0 value appearing in (1) and (2) will be determined in order to avoid inaccurate location results. In addition, different characteristics of the nodes should be taken into account: the use of a unique E_0 value for all the Rx nodes supposes that all of them have the same characteristics (e.g., antenna radiation pattern, radiation efficiency, and antenna adaptation).

Considering these premises, a procedure to calculate E_0 value for each Rx node (which will be referred as calibration coefficients, CC's) is described next.

(1) The coverage area is subdivided in several cells (see Figure 12), whose size should not be larger than 4-5 m, reducing the possibility of RSS values corruption when multipath contributions become as significant as the direct contribution (see Figure 5).

(2) The Tx node is placed inside each cell (position denoted as calibration point, see Figure 12), obtaining a set of RSS measurements.

(3) Being known the Tx position (calibration point coordinates), the measured RSS values on each cell are used to determine a calibration coefficient (CC) for each Rx node and for each cell. The CC's values are proportional to the RSS value deviation with respect to the free space field decay law (see Figure 2).

The described calibration procedure can be seen as a rough fingerprinting technique, as the one described in [5]. Fingerprinting is based on measuring the RSS values in all the points of a grid which covers the ILS deployment area. The method described uses the calibration to reduce the measured RSS values deviation with respect to the free space field decay law. Moreover, the calibration procedure corrects the differences between the location network sensors (antenna gain and adaptation as well as the receivers' sensitivity).

3. Experimental Validation

The proposed RSS-based indoor location method was first evaluated using simulation tools for the prediction of radioelectric coverage in indoor scenarios, as explained in [24]. The next step has been experimental validation using a set of indoor measurements.

The first set of field measurements has been done in the scenario shown in Figure 3. A monopole antenna has been chosen as Tx (see Figure 4), placed at a fixed position ($x = 10\,\mathrm{m}$, $y = 2.5\,\mathrm{m}$). For the Rx system, a commercial omni-directional probe, connected to a portable spectrum analyzed, has been selected (Figure 4). The probe antenna can be easily displaced inside the scenario, allowing fast field acquisitions on different positions.

Regarding the working frequency band, two ISM (industrial, scientific, and medical) bands have been selected: 433 MHz and 2.4 GHz (being the last one coincident with ZigBee devices), and the 868 MHz frequency, which is used for RFID applications and short-range RF communications. It is expected that accurate results will occur for the lowest frequency (433 MHz), as the attenuation and multipath effects increase with the frequency.

First, the proposed free-space model is compared with simulations and measurements. Figure 5 shows the field level along the x-axis being $f = 2450\,\mathrm{MHz}$. Measurements have been done each $\Delta x' = 10\,\mathrm{cm}$ $(0.8\,\lambda)$. It is possible to appreciate a good agreement with the free-space field decay law for those positions close to the Tx position ($R < 3\,\mathrm{m}$).

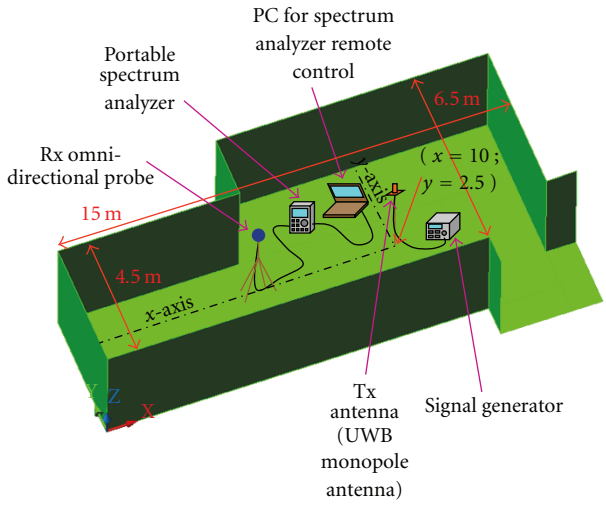

Figure 3: First measurement indoor scenario.

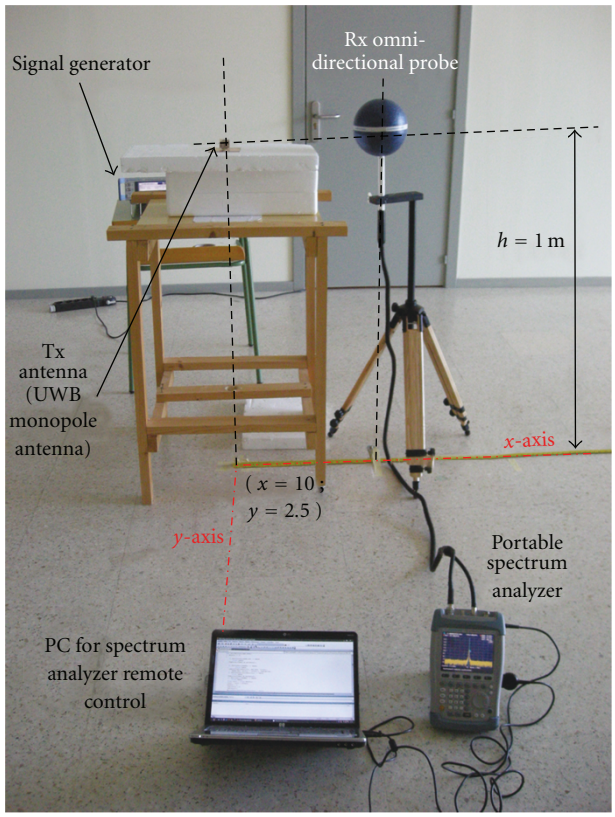

Figure 4: Tx and Rx set-up.

For larger distances ($R > 3$ m), effects of multipath due to reflections in floor and walls appear as fast oscillations on the measured field level.

Next step is the location method accuracy evaluation considering multiple frequencies. Previous results using different measurement subsets on the first scenario were published in [25]. Thus, another indoor scenario (shown in Figure 6) has been selected for this contribution, being its

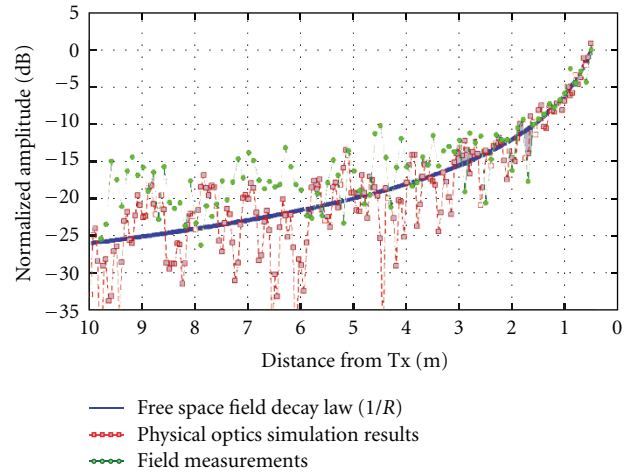

Figure 5: Measured field amplitude (green beacons) versus Tx-Rx distance (along x-axis). Comparison with the theoretical field amplitude assuming free-space conditions (blue line) and Physical Optics simulation of the indoor environment (red beacons).

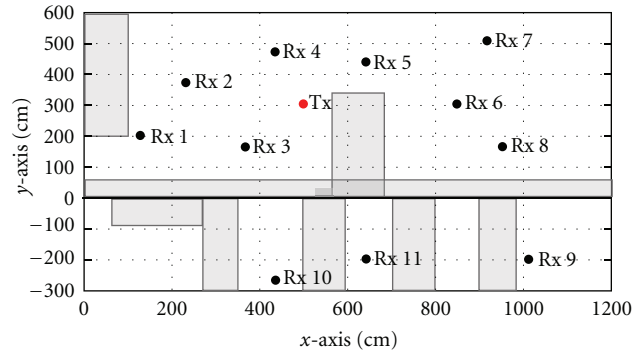

Figure 6: Second measurement indoor scenario. Placement of the Rx (black dots) and the Tx (the red dot). The black line represents a wall, while the rooms' furniture is indicated by grey rectangles.

size 15 m. In this case, 11 different Rx placements have been chosen, being 3 of them in a NLOS situation (9, 10, and 11, see Figure 6). In order to have a significant number of samples, 250 measurements have been collected at each Rx placement within 1 hour period. Also, several uncertainties in the Rx position have been introduced, by displacing the measurement setup (the omnidirectional probe shown in Figure 4) ±0.25 m around the exact Rx position.

Different configurations have been evaluated, analyzing the influence of the number and placement of the Rx, working frequency, and the use of one or multiple frequencies. As an example, Figure 7 represents the ILS evaluation using the measurements taken at Rx positions 1, 4, 5, 6, and 7, and combining the three working frequencies (433, 868, and 2450 MHz). For this case, the Tx mean positioning error is 0.85 m (~ 5.7% of the scenario's size).

Apart from the cost function representation, accuracy analysis can be done by representing the Tx positioning error in an histogram, which is plotted in Figure 8. It is clearly appreciated that the histogram's peak is below 0.75 m

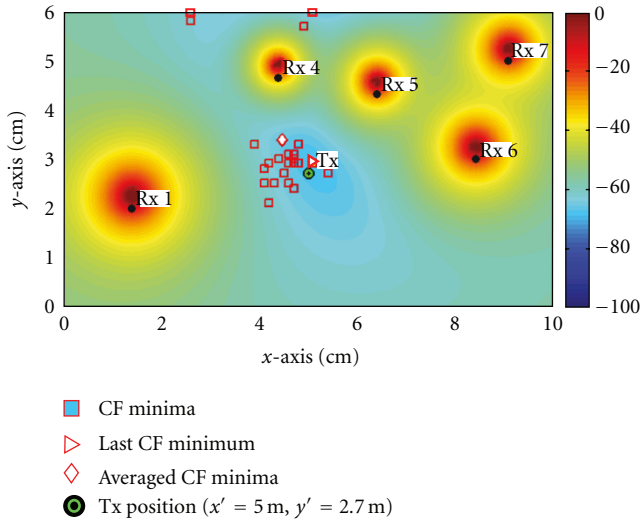

Figure 7: Location system evaluation using field amplitude measurements (combination of the three working frequencies). The colormap represents the amplitude (normalized, in dB) of the cost function (CF) of (3).

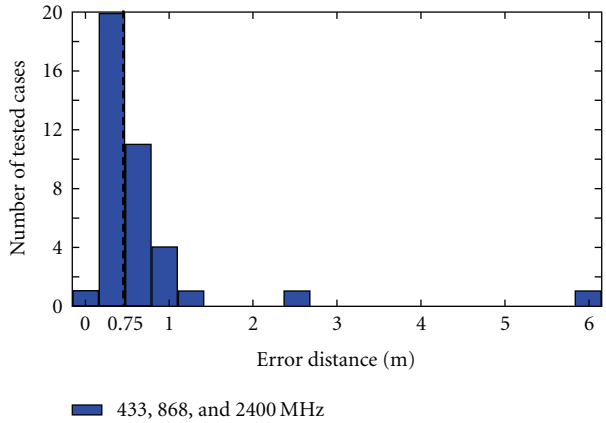

Figure 8: Histogram with the Tx positioning error combining the results of the three frequencies. Number of tested cases: 50 (y-axis is limited to 20 cases).

(5% of the scenario's size). When using just one frequency (Figure 9), the results' dispersion is larger, but the peak is still below 0.75 m for each frequency.

Table 2 reports the averaged error (the location error for the 250 measurements at each Rx is averaged) for 8 configurations with different Rx (placement and number of Rx), LOS and NLOS conditions (NLOS means that there is one or more Rx in this situation with respect to the Tx), and for each working frequency. In most cases, more accurate results are achieved when increasing the number of Rx, by combining the three frequencies results, and when there are no Rx in NLOS situation. Also, from the averaged error reported in Table 2, it can be concluded that the proposed method's accuracy is slightly better than those ones presented in Table 1.

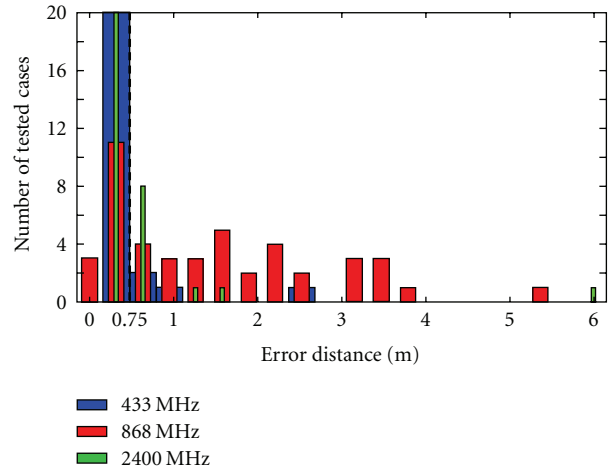

Figure 9: Histogram with the Tx positioning error for each frequency. Number of tested cases: 50 (y-axis is limited to 20 cases).

Table 2: LOS and NLOS accuracy comparison.

Selected Rx	LOS/NLOS	Averaged error (m) Frequency (MHz)			
		433	868	2450	3 freqs.
2,4,5,6,7,8	LOS	0.3	0.8	0.44	0.51
1,3,4,5,6,8	LOS	0.3	1.43	0.54	0.27
1,5,6,7,9,11	NLOS	0.11	1.82	1.12	1.33
2,4,5,7,9,10	NLOS	0.88	0.63	0.32	0.47
1–8	LOS	0.6	0.4	0.39	0.28
1–4,6,7,9,11	NLOS	0.13	1.23	0.28	0.09
4–11	NLOS	0.27	1.36	0.46	0.59
1–11	NLOS	0.34	0.7	0.14	0.2
Mean value of each col.		0.37	1.05	0.46	0.47

To conclude this section, it must be remarked that the measurement setup presented in this section is conceived to provide accurate RSS measurements, so inaccuracies are mainly due to indoor propagation effects (signal attenuation, multipath).

4. ZigBee Implementation

4.1. ZigBee Network Description. Once the proposed RSS indoor location method has been evaluated in real indoor scenarios, a testbed based on a ZigBee network is proposed. The network uses three node types all based on the same 802.15.4 PHY link: a gateway or coordinator node used to interface the ZigBee Network and computer controller, a number of static nodes at known locations and the mobile node attached to the mobile asset. Background coverage for the network is provided by the static nodes, which are located throughout the target area, on a grid of roughly 20 to 30 meters, which gives a minimum coverage network for a building or area.

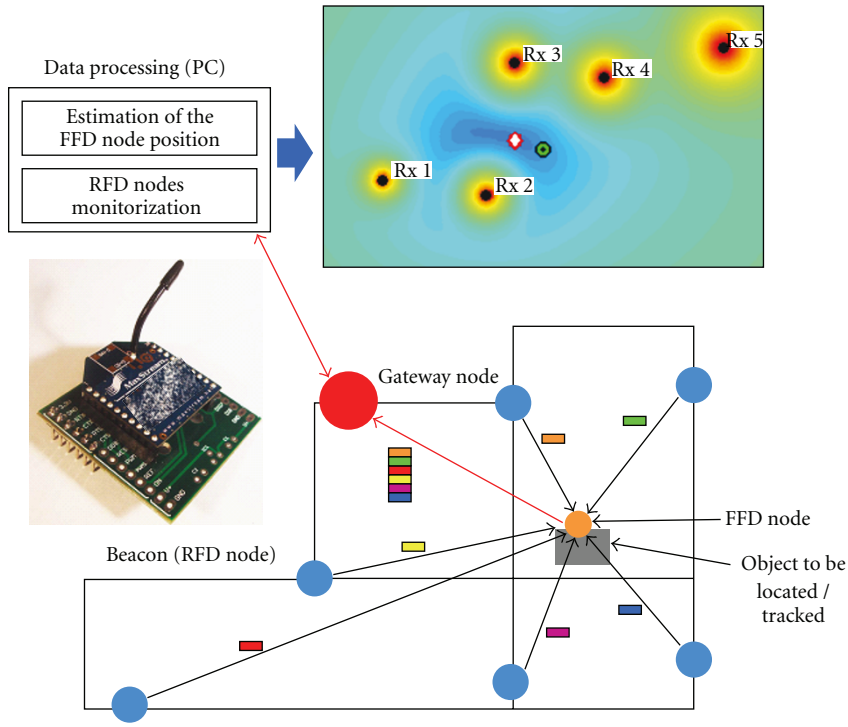

Figure 10: ZigBee-based location network implementation.

ZigBee standard [16] requires RSS indication to be measured accurately for general channel assessment. The interchangeable modules XBee and XBee-PRO [26] from MaxStream are selected because these chips provide RSS indication measurement tagged to a specific packet. The operating frequency is 2.4 GHz, with a 250 Kbps data rate. XBee module provides up to 30 m ranges for indoor and urban environments and up to 100 m for LOS outdoor conditions (with dipole antennas), both for a 1 mW (0 dBm) output transmitted power whereas XBee-PRO module provides, for a 100 mW (20 dBm) output transmitted power, up to 100 m ranges for indoor and urban environments and up to 1200 m for LOS outdoor conditions (with dipole antennas). The method presented in this contribution takes into account the XBee or XBee-PRO features in order to equalize the RSS value. The ZigBee modules are configured to operate in the application programming interface (API) mode, allowing that a host application can configure the modules and interact with their networking capabilities. Concerning software configuration, the static nodes or beacons (Rx nodes) are set as Reduced Function Devices (RFD), and the mobile node (Tx node) is configured as a Full Function Device (FFD).

The proposed ZigBee-based location network configuration is described next. Static nodes (RFD nodes) will be in slept status most of the time (in order to save battery), being periodically awaked to send frames to the mobile node (an FFD node) to be located (also slept most of the time), which forwards the RSS information to the gateway node for calculating mobile node location (see Figure 10). This configuration would simplify the hardware complexity for the static nodes and also reduces the amount of data transferred in the network. For very complex scenarios or distances between mobile and gateway node configurations higher than 100 m, one or various static nodes can be configured as repeaters which resend RSS information from the mobile node to the gateway node.

4.2. ZigBee Nodes Simulation. Prior to the ZigBee-based location network implementation, the proposed location method's performance using simulated RSS values has been evaluated.

The simulated scenario is intended to be similar to the indoor area where the ZigBee nodes are going to be deployed (Section 4.3). The overall dimensions are 8 m × 6 m (i.e., the scenario's size is $D = 10$ m). 5 Rx nodes are considered, whose positions are indicated in Table 3 and plotted in Figure 11.

The ZigBee nodes' limitation with respect to the measurement setup described in Section 3 is that just one frequency (2.45 GHz) is available, being not possible the use of multifrequency information to increase the location method's accuracy. In consequence, the strategy to be adopted in this section will be the scenario division in cells. For this example, two cells of approximately 5 m × 4 m are considered, being the calibration points' coordinates listed in Table 3. Cells' sizes and calibration points are plotted in Figure 11.

First, the location method is calibrated (following the procedure described in Section 2.3). Once the CC's for each node are calculated using the measured RSS at the cell's calibration point, the proposed location method is ready to work. The location method's flowchart is described next.

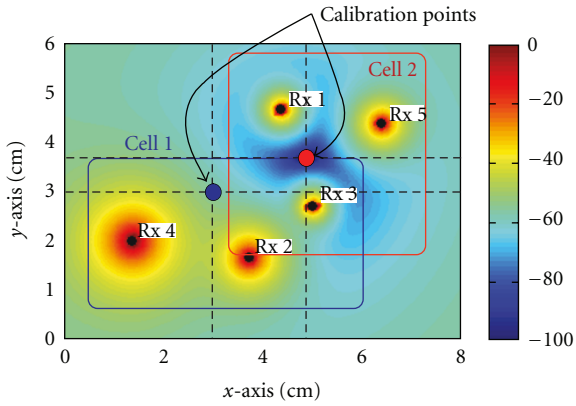

Figure 11: Scenario division in cells and calibration point at each cell. The color scale represents the cost function (3) value (in dB), evaluated at each point of the scenario when the Tx is placed at Cell 2 calibration point.

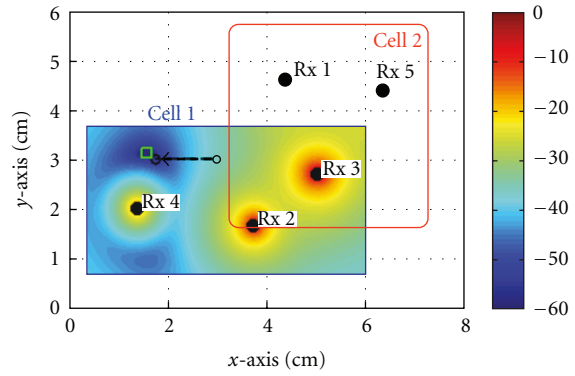

Figure 12: Scenario division in cells makes possible to reduce the search area to the selected cell's size: in this example, the Tx (white square) is estimated to be inside Cell 1. The color scale represents the cost function values inside the Cell 1.

(1) A new set of RSS measurements is calculated each 1 second in all the Rx.

(2) Next, the method estimates the cell (Cell 1 or Cell 2) where the Tx is placed, by looking at the highest RSS values in all the Rx.

(3) RSS measurements are used to compute the cost function, weighting them by the CC's of each Rx node.

(4) The cost function is minimized and the Tx position is estimated, determining again the RSS values deviation with respect to the free space decay law (see Figure 2).

(5) The deviation calculated in (4) is used to discard those nodes that may provide a wrong RSS value (due to multipath effects).

(6) The Tx position is estimated using the RSS values corresponding to the nondiscarded nodes.

At this point it is important to remark again the idea of the scenario division in cells. Apart from the calibration

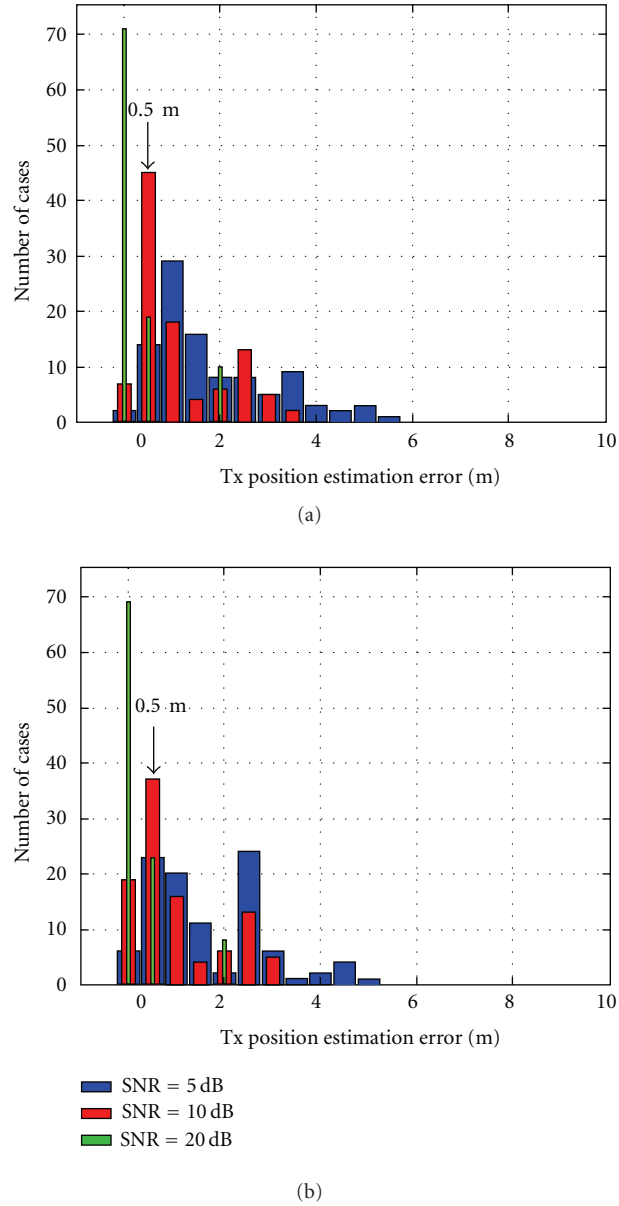

Figure 13: Histograms of the Tx position error for different SNR. (a) Without scenario division in cells. (b) With scenario division in 2 cells.

considerations mentioned at the end of Section 2.3, the goal of the cells is to reduce the area where the cost function is evaluated, as illustrated in Figure 12.

The method's accuracy has been tested in two different positions: Position 1 is $x = 3$ m, $y = 3$ m (green point in Figure 12), and Position 2, $x = 1.75$ m, $y = 3$ m (purple point). Multipath effects and nonstationary conditions of the indoor environment are simulated by adding noise to the simulated RSS values. The signal-to-noise ratio (SNR) is defined at the distance of 1 m from the Tx (free-space field decay law at 1 m, and the effects of the noise in the RSS values are shown in Figure 2).

Table 3: ZigBee nodes and cells placement.

Cell	Node	x (m)	y (m)
2	Rx1	4.37	4.66
1	Rx2	3.72	1.66
1,2	Rx3	5	2.7
1	Rx4	1.38	2
2	Rx5	6.39	4.37
1	Calibration point	3	3
2	Calibration point	5	3.68

Table 4: Tx position error for different configurations.

	SNR at 1 m from the Tx		
	5 dB	10 dB	20 dB
	Mean Tx position error		
No cell division	1.85 m	1.12 m	0.37 m
2 cells	1.70 m	1.02 m	0.34 m
	Standard deviation (σ)		
No cell division	1.26 m	0.93 m	0.55 m
2 cells	1.19 m	0.90 m	0.50 m

Table 4 summarizes the mean Tx position error and the standard deviation (σ) for different SNR values. 50 simulations of RSS values have been carried out at each Tx position (Positions 1 and 2). It has been included a comparison between considering the whole scenario, and the scenario division in 2 cells. It is observed that scenario division improves the location method's accuracy.

To conclude this subsection, the histogram of the Tx position error considering the simulation parameters of Table 4 is plotted in Figure 13. Note that the Tx position error is $\leq$0.5 m in the majority of the simulation cases when the SNR is $\geq$10 dB.

4.3. Measurement Setup. The ZigBee-based location network performance is evaluated in a real scenario shown in Figure 14, previously simulated in Section 4.2. For this experiment, 6 ZigBee nodes are available, one is used as Tx (mobile node), and the other 5 are acting as Rx (static nodes or beacons, see Figure 11). Scenario configuration (Rx positions, number of cells, and calibration points) are the same as these ones used in Section 4.2. As usual, the first step is the location method's calibration by placing the Tx node at the cells' calibration points.

Preliminary results using the proposed ZigBee network infrastructure are shown in Figure 15, where the mobile (Tx) node is displaced from the Position 1 (Figure 15(a)) to the Position 2 (Figure 15(b)), as in the simulation case. The method was able to detect that the Tx node was inside the Cell 1 in both positions. In addition, Rx No. 5 was providing an inaccurate RSS value so it was discarded to calculate the Tx position. The reported location error is below 0.3 m in both points, which is less than 4% of the scenario's size (8 m $\times$ 6 m).

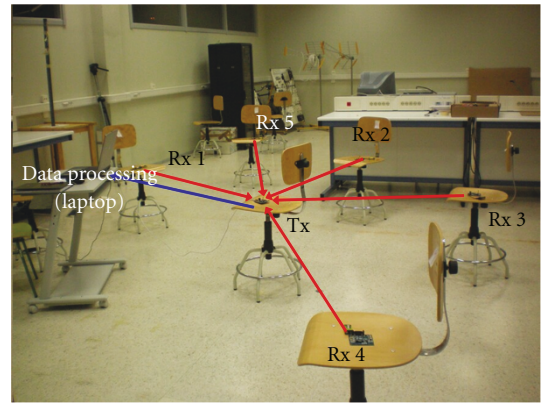

Figure 14: Indoor scenario and placement of the ZigBee nodes.

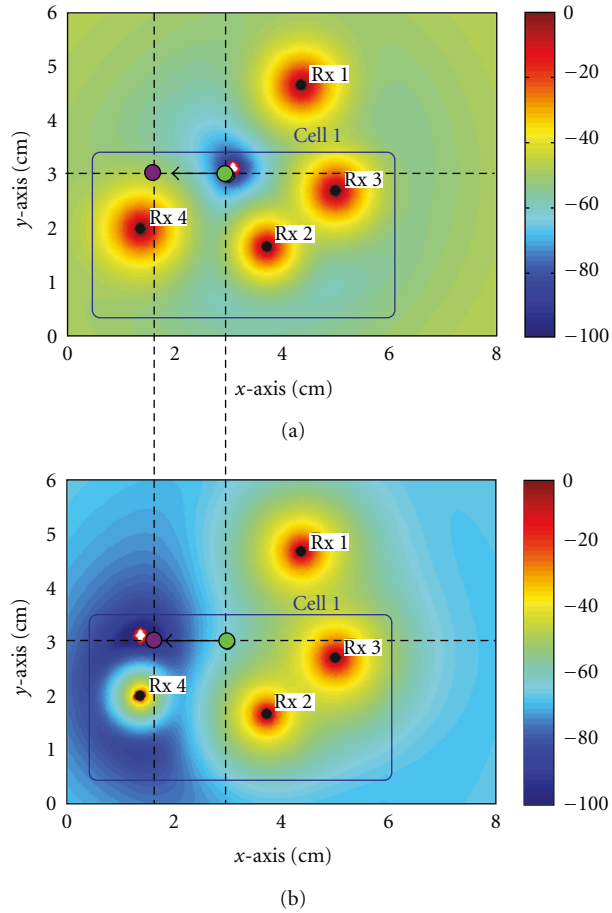

Figure 15: Location method evaluation in Positions 1(a) and 2(b) using RSS measurements from ZigBee nodes. Colormap represents the cost function evaluation at each point of the scenario.

5. Conclusions

A full-wave-based indoor location method has been presented. The proposed technique has been tested in different real indoor scenarios, analyzing the free-space model accuracy in multipath environments. First, an accurate measurement setup was proposed, checking the method's

capabilities for handling multifrequency RSS information, yielding in a more accurate Tx position estimation. Next, the ZigBee-based sensor network was used regarding location method's practical implementation. Despite the fact that multifrequency information is not provided, the lack of accuracy is partially overcome by the scenario division in cells (which reduce the search area) and the use of a calibration procedure based on RSS measurements taken at each cell. Preliminary results using the ZigBee nodes have been presented, highlighting the fact that it is possible to reach the initial accuracy requirement (error less than 5% of the indoor scenario's size).

Acknowledgments

This work has been supported by the "Ministerio de Ciencia e Innovación" of Spain/FEDER" under Projects TEC2008-01638/TEC (INVEMTA) and CONSOLIDER CSD2008-00068 (TERASENSE) and by the "Cátedra Telefónica-Universidad de Oviedo". The authors would like to thank Mr. Manuel Domínguez for his useful help in the measurements and software elaboration and Dr. Jaime Laviada and Dr. Javier Gutiérrez for manufacturing the monopole antenna.

References

[1] H. Liu, H. Darabi, P. Banerjee, and J. Liu, "Survey of wireless indoor positioning techniques and systems," *IEEE Transactions on Systems, Man and Cybernetics Part C*, vol. 37, no. 6, pp. 1067–1080, 2007.

[2] A. Harter and A. Hopper, "Distributed location system for the active office," *IEEE Network*, vol. 8, no. 1, pp. 62–70, 1994.

[3] W. Jung and W. Woo, "Indoor orientation method using ubiTrack," in *Proceedings of the 1st Korean-Japan Joint Workshop on Ubiquitous Computing and Networking Systems*, 2005.

[4] R. Want, A. Hopper, V. Falcao, and J. Gibbons, "Active badge location system," *ACM Transactions on Information Systems*, vol. 10, no. 1, pp. 91–102, 1992.

[5] M. F. Catedra, J. M. Gomez, S.F. Cejudo, and I. Gonzalez, "Application of high frequencies techniques for location systems," in *URSI Commission B EMT-Symposium*, Ottawa, Canada, July 2007.

[6] P. Bahl and V. N. Padmanabhan, "RADAR: an in-building RF-based user location and tracking system," in *Proceedings of the 19th Annual Joint Conference of the IEEE Computer and Communications Societies (INFOCOM '00)*, pp. 775–784, Tel Aviv, Israel, March 2000.

[7] J. Hallberg, M. Nilsson, and K. Synnes, "Positioning with bluetooth," in *Proceedings of the 10th IEEE International Conference on Telecommunications (ICT '03)*, vol. 2, pp. 954–958, March 2003.

[8] J. C. Chen, R. E. Hudson, and K. Yao, "Maximum-likelihood source localization and unknown sensor location estimation for wideband signals in the near-field," *IEEE Transactions on Signal Processing*, vol. 50, no. 8, pp. 1843–1854, 2002.

[9] P. Steggles and G. Schwind, "The ubisense smart space platform advances in pervasive-computing," in *Proceedings of the 3rd International Conference on Pervasive Computing*, vol. 191, Munich, Germany, 2005.

[10] C. Yuechun and A. Ganz, "A UWB-based 3D location system for indoor environments," in *Proceedings of the 2nd International Conference on Broadband Networks (BROADNETS '05)*, vol. 2, pp. 224–232, October 2005.

[11] J. A. Gutierrez, M. Naeve, E. Callaway, M. Bourgeois, V. Mitter, and B. Heile, "IEEE 802.15.4: a developing standard for low-power low-cost wireless personal area networks," *IEEE Network*, vol. 15, no. 5, pp. 12–19, 2001.

[12] P. Ali-Rantala, L. Ukkonen, L. Sydänheimo, M. Keskilammi, and M. Kivikoski, "Different kinds of walls and their effect on the attenuation of radiowaves indoors," in *Proceedings of the IEEE International Antennas and Propagation Symposium (AP-S '03)*, vol. 3, pp. 1020–1023, Columbus, Ohio, USA, June 2003.

[13] C. Wang, H. Wu, and N.-F. Tzeng, "RFID-based 3-D positioning schemes," in *Proceedings of the 26th IEEE International Conference on Computer Communications (INFOCOM '07)*, pp. 1235–1243, Anchorage, Alaska, USA, May 2007.

[14] S. Hara and D. Anzai, "Experimental performance comparison of RSSI-and TDOA-based location estimation methods," in *Proceedings of the 67th IEEE Vehicular Technology Conference (VTC '08)*, pp. 2651–2655, Singapore, May 2008.

[15] IEEE Std 802.15.4-2003, "IEEE Std 802.15.4., Part 15.4: Wireless Medium Access Control (MAC) and Physical Layer (PHY) specification for Low Rate wireless Personal Area Networks (LR-WPANs)," December 2003.

[16] "ZigBee Alliance," http://www.zigbee.org/.

[17] K. Yedavalli, B. Krishnamachari, S. Ravulat, and B. Srinivasan, "Ecolocation: a sequence based technique for RF localization in wireless sensor networks," in *Proceedings of the 4th International Symposium on Information Processing in Sensor Networks (IPSN '05)*, pp. 285–292, Los Angeles, Calif, USA, April 2005.

[18] K. Lorincz and M. Welsh, "MoteTrack: a robust, decentralized approach to RF-based location tracking," *Personal and Ubiquitous Computing*, vol. 11, no. 6, pp. 489–503, 2005.

[19] R. Stoleru and J. Stankovic, "Probability grid: a location estimation scheme for wireless sensor networks," in *Proceedings of the 1st Annual IEEE Communications Society Conference on Sensor and Ad Hoc Communications and Networks (SECON '04)*, Santa Clara, Calif, USA, October 2004.

[20] C. Hyunggi, K. Myungseok, P. Jonghyuk, P. Byungsung, and K. Hagbae, "Performance analysis of location estimation algorithm in ZigBee networks using received signal strength," in *Proceedings of the 21st International Conference on Advanced Information Networking and Applications Workshops (AINAW '07)*, pp. 302–306, can, May 2007.

[21] C. A. Balanis, *Antenna Theory: Analysis and Design*, John Wiley & Sons, New York, NY, USA, 1997.

[22] G. Shen, R. Zetik, O. Hirsch, and R. S. Thomä, "Range-based localization for UWB sensor networks in realistic environments," *EURASIP Journal on Wireless Communications and Networking*, vol. 2010, Article ID 476598, 9 pages, 2010.

[23] W. H. Press, S. A. Teukolsky, W. T. Vetterling, and B. P. Flannery, *Numerical Recipes in C: The Art of Scientific Computing*, Cambridge University Press, Cambridge, UK, 1992.

[24] Y. Álvarez, F. Las-Heras, and M. R. Pino, "Full-wave methods for RF sources location," in *Proceedings of the 2nd European Conference on Antennas and Propagation (EuCAP '07)*, Edinburgh, UK, November 2007.

[25] Y. Álvarez, M. E. de Cos, and F. Las-Heras, "Full-wave-based location system method evaluation," in *IEEE MTT-S International Microwave Workshop on Wire-less Sensing, Local Positioning and RFID*, Cavtat, Croatia, September 2009.

[26] "Product Manual v1.xAx, IEEE 802.15.4 OEM RF Modules," MaxStream, Inc.